ACCOUNTS
of chemical research

Periodic Trends in Organic Functionalization of Group IV Semiconductor Surfaces

JESSICA S. KACHIAN, KEITH T. WONG, AND STACEY F. BENT*

Department of Chemical Engineering, Stanford University, Stanford, California 94305

RECEIVED ON SEPTEMBER 30, 2009

CONSPECTUS

Organic functionalization of group IV semiconductor surfaces provides a means to precisely control the interfacial properties of some of the most technologically important electronic materials in use today. The 2×1 reconstructed group IV (100) surfaces in ultrahigh vacuum, in particular, have a well-defined surface that allows adsorbate−surface interactions to be studied in detail. Surface dimers containing a strong σ- and weak π-bond form upon reconstruction of the group IV (100) surfaces, imparting a rich surface reactivity, which allows useful analogies to be made between reactions at the surface and those in classic organic chemistry.

To date, most studies have focused on single substrates and a limited number of adsorbate functional groups. In this Account, we bring together experimental and theoretical results from several studies to investigate broader trends in thermodynamics and kinetics of organic molecules reacted with group IV (100)-2×1 surfaces. By rationalizing these trends in terms of simple periodic properties, we aim to provide guidelines by which to understand the chemical origin of the observed trends and predict how related molecules or functionalities will react.

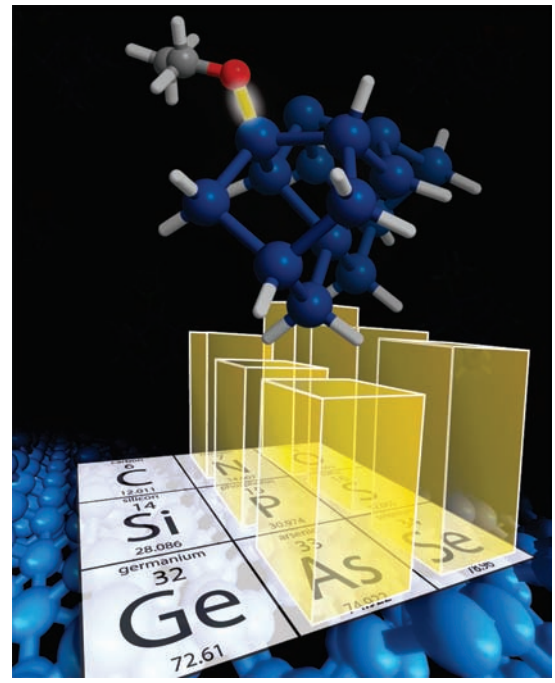

Results of experimental and theoretical studies are used to show that relative electronegativities and orbital overlap correlate well with surface−adsorbate covalent bond strength, while orbital overlap together with donor electronegativity and acceptor electron affinity correlate with surface−adsorbate dative bond strength. Using such simple properties as predictive tools is limited, of course, but theoretical calculations fill in some of the gaps. The predictive power inherent in periodic trends may be put to use in designing molecules for applications where controlled attachment of organic molecules to semiconductor surfaces is needed. Organic functionalization may facilitate the semiconductor industry's transition from traditional silicon-based architectures to other materials, such as germanium, that offer better electrical properties. Potential applications also exist in other fields ranging from organic and molecular electronics, where control of interfacial properties may allow coupling of traditional semiconductor technology with such developing technologies, to biosensors and nanoscale lithography, where the functionality imparted to the surface may be used directly. Knowledge of thermodynamic and kinetic trends and the fundamental basis of these trends may enable effective development of new functionalization strategies for such applications.

Introduction

Over the past several years, increasing attention has been directed toward the organic functionalization of group IV semiconductor surfaces due to potential applications in a number of fields, including molecular electronics, nanoscale lithography,

Published on the Web 12/30/2009 www.pubs.acs.org/acr
10.1021/ar900251s

and biosensors.[1,2] Advances in these and other applications may be achieved by combining current knowledge of microelectronics fabrication with the tailorability afforded by organic materials and the precise interface control that is possible with atomically clean surfaces. Realizing this vision requires a detailed understanding of the chemistry taking place at the semiconductor surface.

A number of studies within our group have focused on understanding the chemistry of organic molecules of varying functionality at group IV (100) surfaces. Upon proper preparation under vacuum, group IV (100) surfaces undergo a 2×1 reconstruction, which entails the formation of surface dimers that possess a strong σ-bond and a weak π-bond.[3] Many recent studies have shown that analogies between the organic functionalization of (100)-2×1 group IV semiconductor surfaces and classic organic chemistry constitute a means for characterizing and understanding these surface reactions.[1,2] The analogy between the surface dimer and a double bond, for example, is shown to be particularly appropriate for the class of attachment reactions known as cycloadditions. Moreover, the dimer tilt present at the Si(100)-2×1 and Ge(100)-2×1 surfaces results in a nucleophilic "up" atom and an electrophilic "down" atom,[4] which can function as a Lewis base and Lewis acid, respectively.[2] Consequently, studies have shown that many molecules adsorb via donation of a lone pair of electrons to the down atom of the dimer, forming a dative-bonded state.[5−11] The precise structure and order observed with these well-characterized surfaces also allows for better approximation of the chemical system by theoretical methods, which we use to corroborate and aid in understanding our experimental data.

By making comparisons between various adsorption systems, we seek a broader perspective that enables trends observed for the reaction of organic molecules at group IV (100)-2×1 surfaces to be explained, within reasonable bounds, by simple periodic properties of the elements such as electronegativity, orbital character and electron affinity. Such understanding then yields predictive powers that may provide guidance in designing molecules to achieve specific functionality at the surface.

In this Account, we explore trends in group IV substrate periodicity; periodic trends down group V and group VI for adsorbates containing N, P, and As and O, S, and Se; and periodicity across the second row of the periodic table by comparing adsorbates containing C, N, and O. We first contrast how the thermodynamics and kinetics of a simple dissociation reaction across a surface dimer vary among the group IV (100)-2×1 surfaces, focusing on N−H dissociation, for which a large body of literature is available. We also compare the strength of dative bonds to Si and Ge, which constitute important intermediates in many mechanisms on these surfaces. The remainder of this Account is focused primarily on the chemistry of Ge(100)-2×1, the surface of choice for our most recent studies. We examine how X−Ge dative bond strength varies for adsorbate atoms, X, from groups V and VI of the periodic table and also investigate the trends down group V and VI in the thermodynamics of intradimer X−H dissociation on Ge(100)-2×1. We conclude our study with an investigation of how the chemical identity within period 2 of the interacting atom, X, in the adsorbate affects thermodynamics of intradimer X−H dissociation, X−Ge ordinary covalent bond strength, and X−Ge dative bond strength.

Group IV (100)-2×1 Substrate Periodicity

The solids formed from the elements in group IV comprise some of the most technologically important electronic materials in use today. They include diamond, an excellent electrical insulator with high thermal conductivity, and Si and Ge, both extremely important semiconductors. The bulk solids of C, Si, and Ge exhibit many structural similarities: all form diamond cubic lattices, and the (100) surface of each undergoes a 2×1 reconstruction under vacuum in which pairs of surface atoms form new bonds. This reconstruction generates rows of surface dimers with each dimer possessing a strong σ-bond and a weaker π-bond.[3] However, important differences exist in the surface structure and surface electronic properties of these three materials. The diamond surface has symmetric dimers with a bond length of approximately 1.4 Å, whereas the Si and Ge surfaces both have larger asymmetric, or tilted, dimers with a bond length of 2.3−2.5 Å.[12−14] The dimer tilt that occurs for Si and Ge creates an uneven distribution of charge within the surface dimer, resulting in an electron-rich, nucleophilic "up" atom and an electron-deficient, electrophilic "down" atom for these surfaces.[4] These geometric and electronic structural differences affect the individual reactivity of these surfaces toward organic molecules.

To compare the reactivity of group IV (100)-2×1 surfaces, we consider N−H dissociation of dimethylamine. DFT-based quantum chemical calculations were used to calculate the energies of critical points along the intradimer reaction pathways on C(100)-2×1, Si(100)-2×1, and Ge(100)-2×1 shown in Figure 1.[7,8] Calculations were performed at the B3LYP level of theory using the Gaussian suite of programs. A mixed basis set scheme employed the 6-311++G(d,p) basis set to describe the surface dimer and adsorbate atoms and the 6-31G(d) basis set to represent the remaining subsurface atoms and termi-

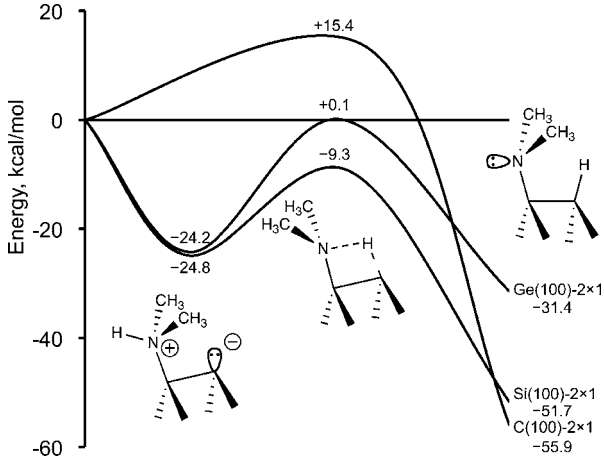

FIGURE 1. Calculated energy diagram for N−H dissociation of dimethylamine on Ge_9H_{12}, Si_9H_{12}, and C_9H_{12} clusters used to represent the respective group IV (100)-2×1 surfaces. All energies are with respect to the reactants in kcal/mol.[7]

nating hydrogens. Figure 1 shows that N−H dissociation of dimethylamine goes through molecularly chemisorbed precursor states on Si(100)-2×1 and Ge(100)-2×1, whereas calculations could find no stable molecularly adsorbed state on C(100)-2×1. This difference can be attributed to the aforementioned dimer tilt on Si(100)-2×1 and Ge(100)-2×1 that allows for electron donation from the adsorbate to the surface down atom to form a dative bond. The symmetry of the C(100)-2×1 dimer, on the other hand, renders molecular adsorption of dimethylamine on C(100)-2×1 unfavorable, as evidenced by the lack of a stable precursor state in Figure 1.

Infrared (IR) spectra of Si(100)-2×1 and Ge(100)-2×1 surfaces exposed to dimethylamine (Figure 2) provide experimental evidence in agreement with the calculated energy diagram in Figure 1. Three main features in the IR spectra of chemisorbed dimethylamine indicate that the molecule undergoes molecular adsorption on germanium and dissociative adsorption on silicon. On Ge(100)-2×1, the chemisorption spectrum lacks absorption in the Ge−H stretching vibration region of 1900−2000 cm^{-1}, retains a peak in the N−H stretching vibration region near 3200 cm^{-1}, and exhibits attenuation of red-shifted C−H Bohlmann bands below 2800 cm^{-1} compared with the multilayer spectrum. These results indicate, respectively, that H has not been transferred to the surface, that the N−H bond of dimethylamine remains intact upon adsorption, and that the N lone pair is no longer present to elongate and, thus, red-shift absorption of the *trans* periplanar C−H bonds by the *trans*-lone-pair effect, which gives rise to the Bohlmann bands. Essentially the opposite results are seen for dimethylamine chemisorbed on Si(100)-2×1. These results indicate that dimethylamine adsorbs molecularly by donation of its lone pair electrons to the Ge(100)-2×1 surface, whereas it undergoes N−H dissociation on Si(100)-2×1. A full analysis of the IR spectral assignments can be found in refs 7 and 8. Although the transition state to N−H dissociation is calculated to be only 0.1 kcal/mol above the energy of the reactants on Ge(100)-2×1, there is a relatively large (24.3 kcal/mol) barrier to dissociation from the dative bonded state. Thus, if significant thermal accommodation occurs at the dative-bonded state, the dissociated product is not expected to form, in accordance with the experimental data. The same process on Si(100)-2×1 has a smaller activation energy (15.5 kcal/mol above the dative-bonded state or 9.3 kcal/mol *below* the energy of the reactants); thus, the calculation results predict that N−H dissociation will occur more readily on Si(100)-2×1, as observed.

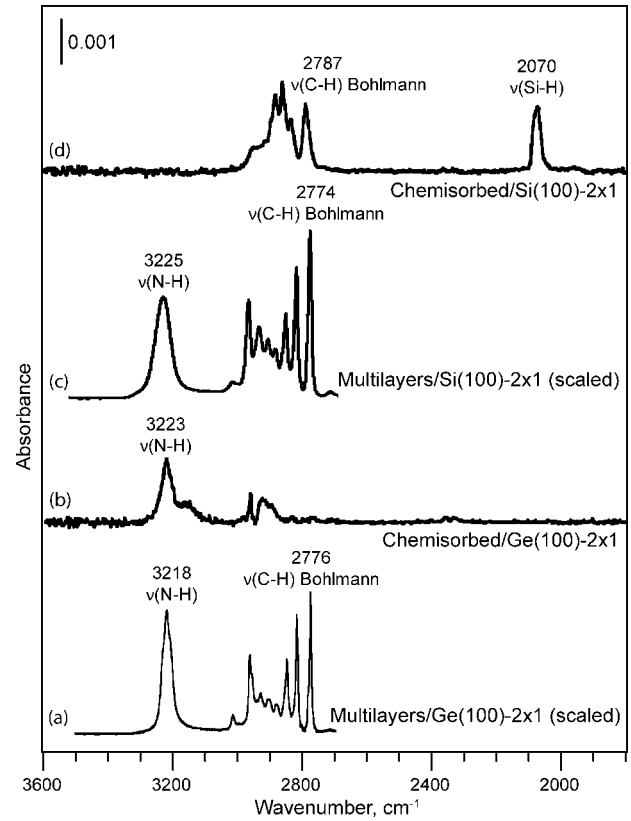

FIGURE 2. Infrared spectra of (a) multilayers of dimethylamine on Ge(100)-2×1 at 120 K, (b) 5 L of dimethylamine chemisorbed on Ge(100)-2×1 at 300 K, (c) multilayers of dimethylamine on Si(100)-2×1 at 100 K, and (d) 100 L of dimethylamine chemisorbed on Si(100)-2×1 at 300 K.[7,8]

The observed difference in reactivity of dimethylamine on Si(100)-2×1 and Ge(100)-2×1 has been previously explained in terms of the difference in proton affinity of the nucleophilic "up" dimer atom. For more details, we refer the reader to refs 7 and 8. Here we focus instead on trends in dative bond energies between these two surfaces. The dative-bonded state is an important intermediate in the N−H dissociation reaction, as

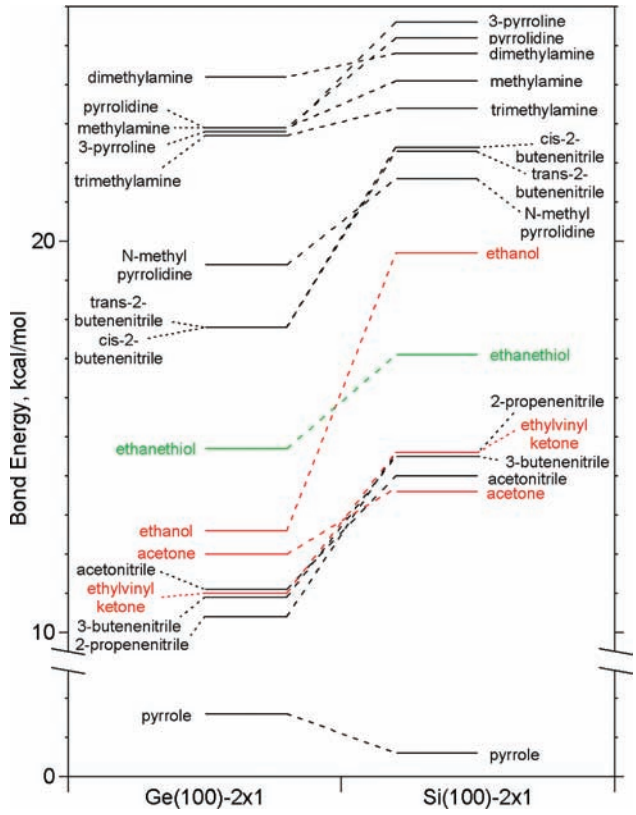

FIGURE 3. Calculated dative bond energies for various adsorbates on Ge(100)-2×1 and Si(100)-2×1 through N (black), O (red), or S (green).[5−11] Dotted lines connect the bond energy for the same molecule on the two surfaces to aid in comparing dative bond strength between Ge(100)-2×1 and Si(100)-2×1.

evident in Figure 1, as well as in many other reactions at these surfaces. By compiling dative bond strengths of a collection of organic molecules with the Si(100)-2×1 and Ge(100)-2×1 surfaces (Figure 3), it is apparent that dative bonds with Si(100)-2×1 are consistently 1−7 kcal/mol stronger than those with Ge(100)-2×1 for any given adsorbate.[15] This trend is observed for the N dative bond of a number of amines and nitriles; the S dative bond of ethanethiol; and the O dative bond of ethanol, acetone, and ethylvinylketone.[5−11]

In general, dative bond strength is affected by both the electronegativity of the donor and the electron affinity of the acceptor. The effect of the donor atom electronegativity will be discussed later. The ability of an atom to accept additional electron density can be loosely related to its electron affinity, which is defined as the negative of the energy change caused by addition of an electron to a neutral atom. For the case of dative bonding on Si(100)-2×1 and Ge(100)-2×1, the reaction involves donation of electron density from the adsorbate to a down dimer atom on the surface, with the Si or Ge substrate acting as the acceptor. The electron affinity of Si (32.0 kcal/mol) is slightly higher than that of Ge (28.4 kcal/mol),[16,17] which may, in part, explain the observed trend of slightly stronger dative bonding on Si(100)-2×1 than Ge(100)-2×1. In addition, orbital overlap also plays a role in determining dative bond strength. Dative bonding involves charge donation from the donor molecule's HOMO to a degenerate LUMO of the group IV (100)-2×1 surface. The larger size of a Ge(100)-2×1 LUMO as compared to a Si(100)-2×1 LUMO may also contribute to the observed trend toward slightly weaker dative bonds on Ge(100)-2×1.

Group V and VI Periodic Trends in Organic Reactivity at Ge(100)-2×1

Studies investigating the reactivity of the Ge(100)-2×1 surface with organic molecules containing heteroatoms from group V or group VI of the periodic table are found throughout the literature.[5,7,18−21] However, the lack of cross-comparison among these studies leaves overarching periodic trends in reactivity of these molecules largely unexplored. Our recent work has highlighted distinct trends in reactivity down group VI by comparing the reactivity of O-, S-, and Se-containing organic molecules with the Ge(100)-2×1 surface.[5] We have also undertaken a series of DFT calculations to supplement the literature for group V heteroatoms. The resulting collection of data provides for new insights into group periodic trends.

Thermodynamics of X−H Dissociation. Considering group VI, DFT and IR results show that ethanol and ethanethiol both adsorb on Ge(100)-2×1 via X−H dissociation at 310 K.[5] Comparison to ethaneselenol, H−Se−CH_2CH_3, is not possible because it is not a stable molecule. DFT-based quantum chemical calculations were used to model both intradimer and interdimer X−H dissociation mechanisms for ethanol and ethanethiol on Ge(100)-2×1.[22] Computational details are given in ref 22. Comparison of the pathways on Ge reveals that the S−H dissociation reaction is ∼7 kcal/mol more exothermic than the corresponding O−H dissociation reaction. Interestingly, this trend is opposite to that for reaction of these molecules on Si(100)-2×1.[23,24]

Thermodynamic insight into the origin of this result is provided by DFT bond energy calculations of bonds broken or formed in the X−H dissociation reactions of ethanethiol and ethanol with the Ge(100)-2×1 surface.[25] Computational details for the bond energy calculations used throughout the paper are provided in ref 25. Scheme 1 displays these reactions, with the bonds broken or formed highlighted in red. Quantitatively, the difference in exothermicity of these reactions is given by

$$\Delta_{O-S,Ge}(\Delta H_{rxn}) = (BE_{O-H} - BE_{O-Ge}) - (BE_{S-H} - BE_{S-Ge}) \quad (1)$$

SCHEME 1. Overall Chemical Reaction for X−H Dissociation across a Ge Dimer[a]

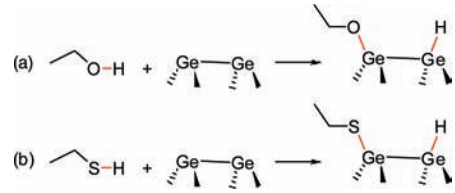

[a] (a) O−H dissociation of ethanol; (b) S−H dissociation of ethanethiol. The germanium surface is represented by a germanium dimer, the fundamental reactive unit in these reactions.

TABLE 1. Results from DFT Bond Energy Calculations[a]

group V		group VI	
bond	energy (BE), kcal/mol	bond	energy (BE), kcal/mol
N−H	94.6	O−H	97.0
P−H	77.0	S−H	81.4
N−Ge	60.3	O−Ge	68.5
P−Ge	50.8	S−Ge	59.4
$\Delta_{N-P,Ge}(\Delta H_{rxn}) = 8.1$ kcal/mol		O−Si	84.0
		S−Si	64.7
		$\Delta_{O-S,Ge}(\Delta H_{rxn}) = 6.5$ kcal/mol	
		$\Delta_{O-S,Si}(\Delta H_{rxn}) = -3.7$ kcal/mol	

[a] Bond energies are given for bonds broken or formed during the X−H dissociation reactions of methylamine and methylphosphine on the Ge(100)-2×1 surface, and ethanol and ethanethiol on the Ge(100)-2×1 and Si(100)-2×1 surfaces. The calculated enthalpy difference $\Delta_{N-P,Ge}(\Delta H)$ between the methylamine and methylphosphine reactions on Ge and between the ethanol and ethanethiol reactions on Ge, $\Delta_{O-S,Ge}(\Delta H)$, and Si, $\Delta_{O-S,Si}(\Delta H)$, are also included.[25]

where BE refers to the bond energy, which is positive by definition. Note that in determining the difference in exothermicity between reactions a and b, bonds broken or formed in both reactions (i.e., Ge−Ge and Ge−H) can be neglected. Calculated bond energies relevant to O−H and S−H dissociation on Ge, and analogous energies for Si, are displayed in Table 1, together with $\Delta_{O-S}(\Delta H_{rxn})$ values obtained using eq 1 for both Ge and Si surfaces.[25] Using the calculated bond energies, the resulting value for $\Delta_{O-S}(\Delta H_{rxn})$ on Ge (6.5 kcal/mol) agrees well with that determined using the larger scale DFT calculations (∼7 kcal/mol). The source of the $\Delta_{O-S}(\Delta H_{rxn})$ result can be understood by considering the calculated values for the bond energies of which it is comprised. According to Table 1, the O−Ge bond formed in the reaction of ethanol is stronger than the S−Ge bond formed in the reaction of ethanethiol by 9.1 kcal/mol; however, the O−H bond, which must be broken, is stronger than the S−H bond by 15.6 kcal/mol. Therefore, the S−H dissociation reaction on Ge(100)-2×1 is thermodynamically more favorable than the corresponding O−H dissociation reaction not because of the strength of the S−Ge bond relative to that of the O−Ge bond but rather because of the weakness of the S−H bond relative to that of the O−H bond.

SCHEME 2. Overall Chemical Reaction for X−H Dissociation across a Ge Dimer, where X Is an Atom from Group V[a]

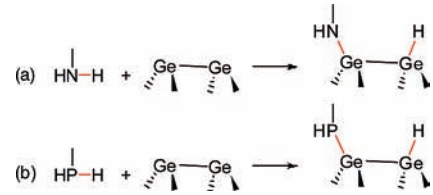

[a] (a) N−H dissociation of methylamine; (b) P−H dissociation of methylphosphine.

Although thermodynamics favor S−H dissociation over O−H dissociation on Ge, this thermodynamic favorability is reversed on Si. The bond energy calculations for O−H and S−H dissociation of ethanol and ethanethiol, respectively, on Si (Table 1) show that O−H dissociation is 3.7 kcal/mol more exothermic than S−H dissociation, consistent with the trend reported in the literature.[23,24] The effect is attributed to the significantly greater strength of the O−Si bond than that of the S−Si bond.

While the literature contains several in-depth theoretical and experimental studies of the reaction of amines with Ge(100)-2×1,[7,11,26] the studies conducted for phosphine reaction with Ge(100)-2×1 are limited and inconsistent with one another.[20,21] Therefore, to investigate the thermodynamic favorability for group V of N−H relative to P−H dissociation on Ge, we have completed DFT bond energy calculations for the X−H dissociation reactions of methylamine and methylphosphine on the Ge(100)-2×1 surface.[25] These reactions are shown in Scheme 2, and the bond energy values are given in Table 1 together with the $\Delta_{N-P,Ge}(\Delta H_{rxn})$ value determined from the bond energies.

Bond energy calculations analogous to those for group VI show that the P−H dissociation reaction is more exothermic (by ∼8 kcal/mol) than the N−H dissociation reaction on Ge(100)-2×1. This result mirrors that for group VI X−H dissociation on Ge. Further, as with group VI, the thermodynamics of group V X−H dissociation are dominated by the difference in bond energies of the bonds broken: although the N−Ge bond is stronger than the P−Ge bond by 9.5 kcal/mol, the P−H bond is weaker than the N−H bond by 17.6 kcal/mol.

Ordinary Covalent X−Ge Bond Strength. The ordinary covalent X−Ge bond strengths (where X is a group V or group VI heteroatom) have been calculated using DFT for rows 2−4 of the periodic table.[25] The results, summarized in Figure 4, show a clear trend toward smaller bond energies down the group.

The decrease in ordinary covalent X−Ge bond strength down groups V and VI of the periodic table is consistent with

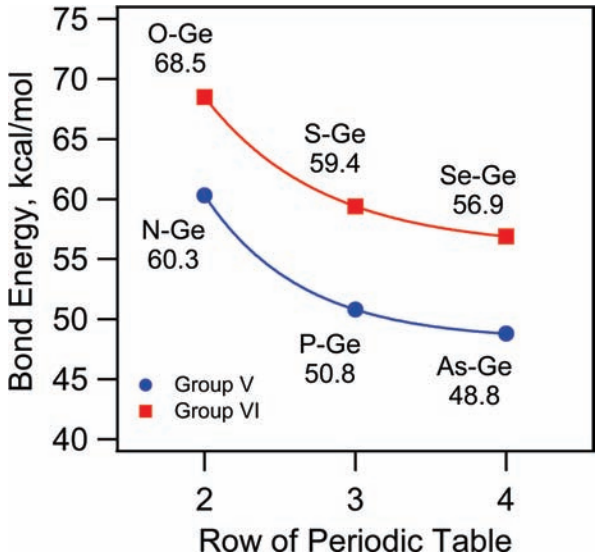

FIGURE 4. X−Ge ordinary covalent bond energies (X = O, S, Se, N, P, As) calculated by DFT for group V and group VI elements. Computational details are provided in ref 25. To guide the eye, a curve has been drawn through each set of points.

the expected periodic trend in these groups. Two important atomic properties that affect covalent bond strength are orbital size and electronegativity. The covalent X−Ge bond between the adsorbate and the germanium surface is formed by overlap primarily between one of the degenerate LUMOs of the surface and the HOMO of the adsorbate, according to DFT calculations. The HOMO of the adsorbates resembles the valence p orbitals of the group V or VI atom on which it is localized. These orbitals increase in size down the group, changing from 2p to 3p to 4p moving from the second to the third to the fourth row atoms. As a result of the increase in adsorbate HOMO orbital size down groups V and VI, X−Ge bond length increases down groups V and VI, respectively. DFT calculations show that the X−Ge bond lengths in the CH_3CH_2X−$Ge(GeH_3)_3$ molecule are 1.83, 2.27, and 2.41 Å for X = O, S, and Se, respectively. The longer bond lengths are accompanied by reduced orbital overlap between X and Ge atoms, resulting in a weaker covalent bond.

Another factor reducing ordinary covalent X−Ge bond strength down groups V and VI is electronegativity. The strength of ordinary covalent bonds is dependent upon the relative electronegativities of the atoms forming the bond. Electronegativity decreases with increasing atomic number down groups V and VI. The Pauling electronegativities of Ge, O, S, and Se atoms are 2.01, 3.44, 2.58 and 2.55, respectively.[27] Consequently, the difference in Pauling electronegativity between oxygen and germanium (1.43) is almost three times larger than either that between sulfur and germanium (0.57) or that between selenium and germanium (0.54). This trend also favors a decrease in ordinary covalent X−Ge bond strength down group VI, and the same trend is found for group V. Consequently, both the poorer orbital overlap and smaller electronegativity difference lead to a decrease in ordinary covalent X−Ge bond strength down groups V and VI, respectively.

The downshift of the group V from the group VI data in Figure 4 indicates that, for X atoms in the same period, the group V X−Ge bond is approximately 8−9 kcal/mol weaker than the group VI X−Ge bond. Since the extent of orbital overlap between X atoms of the same period and Ge should be similar, the greater strength of group VI versus group V ordinary covalent X−Ge bond appears to result from the larger difference in electronegativity between the group VI atom and Ge versus that between the group V atom and Ge.

Dative X−Ge Bond Strength. Unlike with ordinary covalent bonds, for which the periodic properties of orbital size and electronegativity work in concert to favor a higher bond strength for the lighter group V or group VI atom, these properties exert opposite effects on dative bond strength. As with the ordinary covalent bond, the orbital on the molecule involved in formation of the dative bond is the HOMO, which resembles the valence p orbitals of the group V or group VI atom on which it is localized. This orbital is occupied by a lone pair of electrons that donate electron density to the electrophilic Ge surface atom. Down groups V and VI, the increase in HOMO orbital size should reduce orbital overlap with a degenerate LUMO of the Ge surface, leading to a reduction in X−Ge bond strength down the group. However, electronegativity favors dative bonding by the least electronegative donor atom since the electron donor provides both electrons, and a less electronegative X atom is more able to share electrons with other atoms. Therefore, it follows that dative bond strength is negatively correlated with electronegativity of the donating atom. It is the overall trade-off between the effects of X electronegativity and X−Ge orbital overlap that determines trends in X−Ge dative bond strength down groups V and VI of the periodic table.

The study of ether and sulfide functional groups a means to experimentally probe O−Ge and S−Ge dative bond strengths, respectively, for group VI. IR results show that diethyl ether and diethyl sulfide both adsorb via dative bonding for temperatures up to approximately 250 and 340 K, respectively, above which the dative-bonded molecules molecularly desorb.[5] Figure 5 shows the normalized average IR peak area as a function of temperature for both molecules. By the analysis described in ref 5, the data can be fit to an expres-

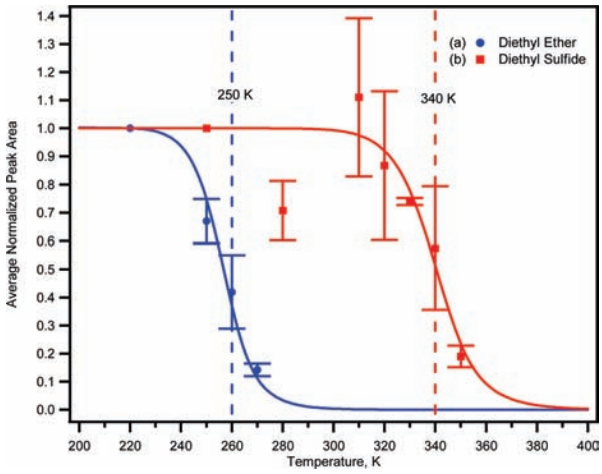

FIGURE 5. Average normalized IR peak area versus temperature for (a) diethyl ether and (b) diethyl sulfide on Ge(100)-2×1. Modes at 1146, 1281, and 1464 cm^{-1} in the diethyl ether spectra and at 1377 and 1451 cm^{-1} in the diethyl sulfide spectra were used in the respective analyses. In each case, these representative modes had consistently high relative intensity in the spectra. Error bars indicate one standard deviation.[5]

sion derived from isothermal desorption kinetics that allows the binding energy to be determined.

From this procedure, the dative bond strengths of diethyl ether and diethyl sulfide with Ge(100)-2×1 are estimated to be 17.9 and 23.8 kcal/mol, respectively, indicating that the S−Ge dative bond of diethyl sulfide is 5.9 kcal/mol stronger than the O−Ge dative bond of diethyl ether.

DFT-calculated[22] X−Ge dative bond strengths for diethyl ether, diethyl sulfide, and diethyl selenide (displayed in Figure 6) are consistent with the experimental data for O−Ge and S−Ge dative bond strengths.[5] Moreover, a comparison of X−Ge dative bond energies (X = O, S, or Se) shows that whereas X−Ge ordinary covalent bond strength *decreases* down group VI (Figure 4), X−Ge dative bond strength *increases* down group VI (Figure 6). As discussed above, the opposite trends are attributed to the different role that electronegativity plays in affecting dative versus ordinary covalent bond strength. Oxygen (Pauling electronegativity of 3.44) is much more electronegative than sulfur (2.58), which, in turn, is slightly more electronegative than selenium (2.55). This suggests that if other effects were unimportant, selenium would form the strongest dative bonds with the germanium surface, followed closely by sulfur, then more distantly by oxygen, as found in this study. Thus, the effect of electronegativity apparently dominates the relative dative bond strength for this system.

Figure 6 also displays DFT results for X−Ge dative bond strength down group V for dimethylamine, dimethylphosphine, and dimethylarsine.[22] The calculations indicate that the

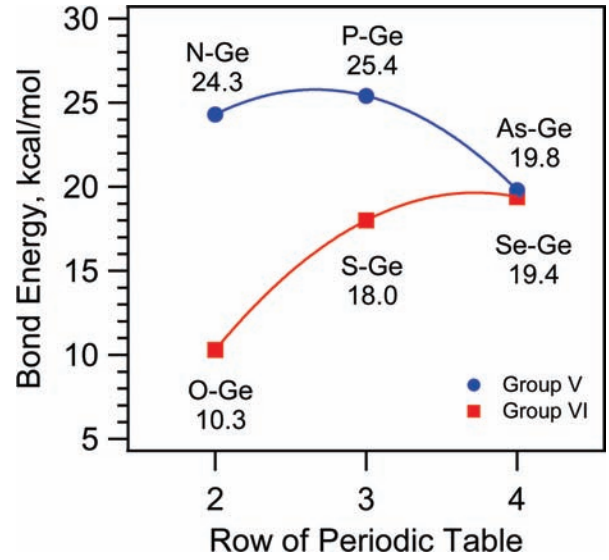

FIGURE 6. X−Ge dative bond energies (X = O, S, Se, N, P, As) calculated by DFT using the $Ge_{15}H_{16}$ cluster to model the Ge(100)-2×1 surface. For X = O, S, or Se, the X atom is part of the $H_3CH_2CXCH_2CH_3$ molecule, whereas for X = N, P, or As, the X atom is part of the $HX(CH_3)_2$ molecule. Additional computational details are provided in ref 22. To guide the eye, a curve has been drawn through each set of points.

P−Ge dative bond is stronger than the N−Ge dative bond by a small amount (1.1 kcal/mol) within error of the calculation, whereas the As−Ge dative bond is approximately 4−5 kcal/mol *weaker* than the N−Ge and P−Ge dative bonds. The lower electronegativity of P (2.19) versus N (3.04) appears to energetically compensate for the longer P−Ge (2.40 Å) versus N−Ge (2.15 Å) dative bond, yielding approximately equal N−Ge and P−Ge dative bond strengths. On the other hand, the electronegativities of P (2.19) and As (2.18) are similar, implying that orbital overlap dominates, with poorer overlap in the case of the larger As atom leading to a weaker dative bond for As than P.

Period 2 Trends in Organic Reactivity at Ge(100)-2×1

This section focuses on thermodynamic trends for adsorbates that react at the Ge(100)-2×1 surface through the period 2 elements of carbon, nitrogen, and oxygen.

To compare the thermodynamics of dissociation on Ge(100)-2×1, we consider intradimer α-C−H, N−H, and O−H dissociation of pyrrole, dimethylamine, and ethanol, respectively. These reactions were modeled using DFT cluster calculations as parts of three separate studies performed by our group; the results are summarized in Table 2.[5,7,11] Although pyrrole is aromatic, its aromaticity is preserved in the C−H dissociated state, and aromaticity appears to affect bond strengths of the broken C−H and formed Ge−C bonds equiv-

TABLE 2. Calculated Energy of Dissociated State (Relative to the Reactants) of Pyrrole, Dimethylamine and Ethanol on Ge(100)-2×1[a]

molecule	dissociated bond	ΔH_{rxn}, (kcal/mol)	surface cluster	basis sets
pyrrole	α-C−H	−32.2	$Ge_2Si_7H_{12}$	dimer and adsorbate, 6-311++G(d,p); subsurface, 6-31G(d)
dimethylamine	N−H	−31.4	Ge_9H_{12}	dimer, adsorbate, and subsurface, 6-311++G(d,p)
ethanol	O−H	−33.0	$Ge_{15}H_{16}$	dimer and adsorbate, 6-311++G(d,p); subsurface, LANL2DZ

[a] All calculations were performed at the B3LYP level of theory.

alently, as indicated by the bond energy calculations described below. Thus, the influence of aromaticity cancels out when ΔH_{rxn} is considered. Interestingly, the exothermicities of the three dissociation reactions presented in Table 2 differ by less than 2 kcal/mol from each other, which is within the error of the calculations. Moreover, similar ΔH_{rxn} values have been calculated for C−H dissociation of formaldehyde (−30.6 kcal/mol), CH_2−H dissociation of *N*-methylpyrrole (−29.4 kcal/mol), and N−H dissociation of pyrrolidine, 3-pyrroline, pyrrole, ethylenediamine, ethylamine, and allylamine (−33.0, −32.7, −34.3, −33.0, −31.6, and −31.7 kcal/mol, respectively) on Ge(100)-2×1.[11,26,28,29]

Bond energies are useful in understanding why the energetics of X−H dissociation on Ge(100)-2×1 are so similar when X is interchanged between C, N, and O. Following the method that was introduced earlier, we can write an equation for the difference in exothermicity of two reactions, $\Delta(\Delta H_{rxn})$, as

$$\Delta_{N-O,Ge}(\Delta H_{rxn}) = (BE_{N-H} - BE_{N-Ge}) - (BE_{O-H} - BE_{O-Ge}) \quad (2)$$

where eq 2 compares N−H and O−H dissociation. Relevant bond energies calculated for pyrrole, dimethylamine, and ethanol using DFT are displayed in Figure 7, in which $\Delta(\Delta H_{rxn})$ is represented visually by comparing the vertical distance between X−H and Ge−X bond energies.[25] It is apparent that despite large differences in absolute bond energies, the energy *differences* are quite similar, explaining why the X−H dissociation reactions of pyrrole, dimethylamine, and ethanol on Ge have similar ΔH_{rxn} values.

Figure 8 compiles the calculated dative bond strengths of a collection of organic molecules dative bonded to the Ge(100)-2×1 surface through C, N, or O.[5−7,9−11,18,19,28−32] There is much overlap in the range of dative bond strengths for molecules bonded through N or O, because dative bond strength is influenced by the nature of the entire molecule (e.g., identity of the functional group containing the dative-bonded atom, and steric, inductive, or resonance effects of

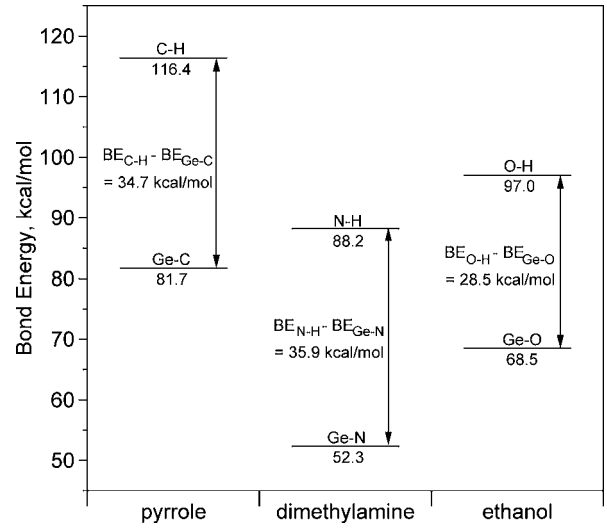

FIGURE 7. Calculated X−H and Ge−X bond energies (X = C, N, O) for pyrrole, dimethylamine, and ethanol.[25]

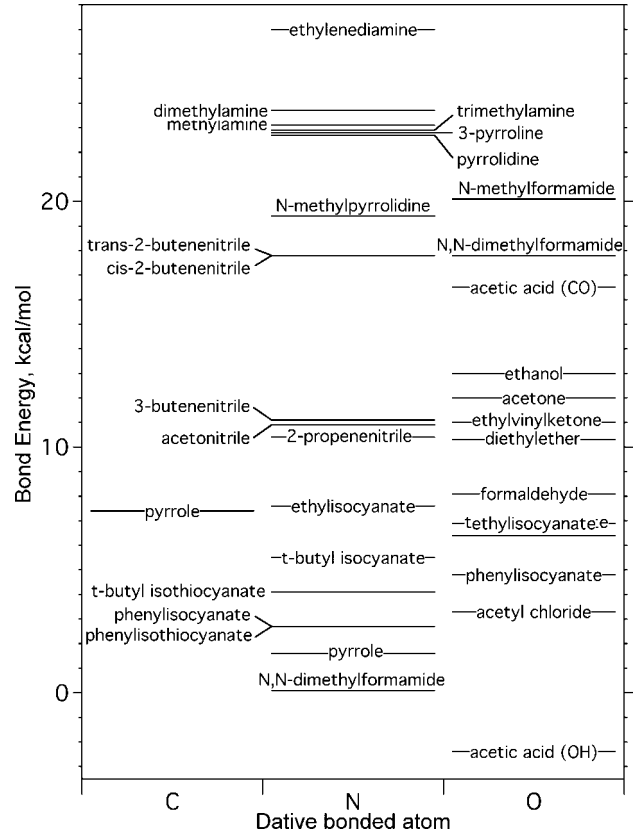

FIGURE 8. Calculated dative energies for various adsorbates dative bonded to Ge(100)-2×1 through C, N, or O.[5−7,9−11,18,19,28−32]

substituents) and not solely determined by the properties of the dative-bonded atom. However, by drawing comparisons between related molecules, the effects of the dative-bonded atom may be isolated, and conclusions about periodic trends in dative bonding can be reached. For example, the N−Ge dative bond between methylamine and Ge(100)-2×1 (23.1 kcal/mol) is 10.1 kcal/mol stronger than the O−Ge dative

bond between ethanol and the same surface (13.0 kcal/mol). Likewise, dimethylamine, trimethylamine, 3-pyrroline, pyrrolidine, and *N*-methylpyrrolidine exhibit N−Ge dative bonds 6−11 kcal/mol stronger than the O−Ge bond through ethanol. The Pauling electronegativity of N (3.04) is considerably smaller than that of O (3.44), so N should be a better electron donor than O in the dative-bonded state on Ge, consistent with the observation of a stronger dative bond.

Another example is pyrrole, which may aptly be used to compare C−Ge and N−Ge dative bond strengths. According to Figure 8, the C−Ge dative bond is 5.8 kcal/mol stronger than the N−Ge dative bond. As before, electronegativity of the donating atom may be considered the driving force behind the observed trend, since the smaller Pauling electronegativity of C (2.55) allows it to share electrons more effectively in a dative bond.

Concluding Remarks

While the majority of studies in the field of dry functionalization of semiconductors have focused on a single substrate or functional group, in this Account we make cross-comparisons among multiple studies to look for broader trends in thermodynamics and kinetics of group IV-, V-, and VI-containing molecules reacted with group IV (100)-2×1 surfaces. Rationalizing the observed behavior on the basis of periodic trends of simple atomic properties such as electronegativity and orbital character provides an understanding of its chemical origin and a means to predict the relative reactivities of similar molecules. In conjunction with experimental results and DFT cluster calculations, bond energy calculations using small, easily modeled clusters are useful for helping to understand and predict thermodynamic trends of even dissimilar organic molecules reacted with the Si(100)-2×1 and Ge(100)-2×1 surfaces.

We find trends toward stronger dative bonding on Si than on Ge and toward an increase in X−Ge dative bond strength down group VI and to the left across period 2 of the periodic table. These results can all be rationalized in terms of donor atom electronegativity, acceptor atom electron affinity, and orbital overlap between the bonding atoms. On the other hand, ordinary covalent X−Ge bond strength decreases down groups V and VI. Electronegativity difference and orbital overlap between the bonding atoms are used to explain these trends.

The predictive power of atomic properties and bond energy calculations may be useful as the semiconductor industry moves away from traditional materials. As improved performance by scaling of Si-based devices is quickly becoming unfeasible, much recent work has focused on alternative materials for use in metal-oxide-semiconductor field-effect transistors. Ge, for example, has higher intrinsic carrier mobilities at room temperature than Si and, thus, may provide a means for improved performance without further reduction of device dimensions. However, Ge does not form a stable passivating oxide like Si, thus prompting the need for an alternative passivating layer, which may be achieved by attachment of organic molecules. Understanding the factors influencing attachment of organics to semiconductor surfaces may aid in transitioning from Si- to Ge-based devices and provide guidance in designing passivating layers for Ge.

Applications of organic functionalization of semiconductors also extend to a number of other fields including organic and molecular electronics, renewable energy, and biosensors. Organic electronics are of intense interest at present due to their potential to bring lower cost, flexible substrates, and biocompatibility to the electronics industry, while Si-based electronics maintain an advantage in terms of performance. In the field of renewable energy, the performance of many developing solar technologies is strongly affected by interfacial phenomena such as electron−hole recombination at interfaces. Chip-based biological and chemical sensors may be made by attachment of organic molecules, providing molecular recognition, to a semiconductor surface, providing well-developed architecture and fabrication technology. All of these potential applications require precise control of interfacial properties. The tailorability of organic molecules provides such control, while understanding the factors that influence reaction of organics with semiconductor surfaces enables these molecules to be attached to the surface as desired.

This work was supported by the National Science Foundation (Grants CHE 0615087 and CHE 0910717).

BIOGRAPHICAL INFORMATION

Jessica S. Kachian received her B.S. in Chemistry and her B.S. in Chemical Engineering from University of Lousiana at Lafayette in 2003 and is currently a graduate student at Stanford University.

Keith T. Wong received his B.S. in Chemical Engineering from Cornell University in 2008 and is currently a graduate student at Stanford University.

Stacey F. Bent is Professor of Chemical Engineering at Stanford University. She received her B.S. in Chemical Engineering from U.C. Berkeley and her Ph.D. in Chemistry from Stanford University. Her research interests are in understanding surface and interfacial chemistry and materials processing and applying this knowledge to problems in semiconductor processing, nanotechnology, and sustainable energy.

REFERENCES

1 Bent, S. F. Organic functionalization of group IV semiconductor surfaces: Principles, examples, applications, and prospects. *Surf. Sci.* **2002**, *500*, 879–903.

2 Filler, M. A.; Bent, S. F. The surface as molecular reagent: Organic chemistry at the semiconductor interface. *Prog. Surf. Sci.* **2003**, *73*, 1–56.

3 Kubby, J. A.; Boland, J. J. Scanning tunneling microscopy of semiconductor surfaces. *Surf. Sci. Rep.* **1996**, *26*, 61–204.

4 Kubby, J. A.; Griffith, J. E.; Becker, R. S.; Vickers, J. S. Tunneling microscopy of Ge(001). *Phys. Rev. B* **1987**, *36*, 6079–6093.

5 Kachian, J. S.; Bent, S. F. Sulfur versus oxygen reactivity of organic molecules at the Ge(100)-2×1 surface. *J. Am. Chem. Soc.* **2009**, *131*, 7005–7015.

6 Mui, C.; Filler, M. A.; Bent, S. F.; Musgrave, C. B. Reactions of nitriles at semiconductor surfaces. *J. Phys. Chem. B* **2003**, *107*, 12256–12267.

7 Mui, C.; Han, J. H.; Wang, G. T.; Musgrave, C. B.; Bent, S. F. Proton transfer reactions on semiconductor surfaces. *J. Am. Chem. Soc.* **2002**, *124*, 4027–4038.

8 Mui, C.; Wang, G. T.; Bent, S. F.; Musgrave, C. B. Reactions of methylamines at the Si(100)-2×1 surface. *J. Chem. Phys.* **2001**, *114*, 10170–10180.

9 Wang, G. T.; Mui, C.; Musgrave, C. B.; Bent, S. F. Example of a thermodynamically controlled reaction on a semiconductor surface: Acetone on Ge(100)-2×1. *J. Phys. Chem. B* **2001**, *105*, 12559–12565.

10 Wang, G. T.; Mui, C.; Musgrave, C. B.; Bent, S. F. Competition and selectivity of organic reactions on semiconductor surfaces: Reaction of unsaturated ketones on Si(100)-2×1 and Ge(100)-2×1. *J. Am. Chem. Soc.* **2002**, *124*, 8990–9004.

11 Wang, G. T.; Mui, C.; Tannaci, J. F.; Filler, M. A.; Musgrave, C. B.; Bent, S. F. Reactions of cyclic aliphatic and aromatic amines on Ge(100)-2×1 and Si(100)-2×1. *J. Phys. Chem. B* **2003**, *107*, 4982–4996.

12 Kruger, P.; Pollmann, J. Dimer reconstruction of diamond, Si, and Ge (001) surfaces. *Phys. Rev. Lett.* **1995**, *74*, 1155–1158.

13 Shirasawa, T.; Mizuno, S.; Tochihara, H. Structural analysis of the c(4 × 2) reconstruction in Si(001) and Ge(001) surfaces by low-energy electron diffraction. *Surf. Sci.* **2006**, *600*, 815–819.

14 Yang, C.; Kang, H. C. Geometry of dimer reconstruction on the C(100), Si(100), and Ge(100) surfaces. *J. Chem. Phys.* **1999**, *110*, 11029–11037.

15 Pyrrole is the one exception on Figure 3 for which a stronger dative bond to the Ge(100)-2×1 surface than the Si(100)-2×1 surface has been calculated. The very weak dative bond of pyrrole has been attributed to the loss of resonance stabilization energy upon dative bonding. This may also affect the relative strengths of dative bonding to the two surfaces.

16 Blondel, C.; Delsart, C.; Goldfarb, F. Electron spectrometry at the μeV level and the electron affinities of Si and F. *J. Phys. B* **2001**, *34*, L281–L288.

17 Scheer, M.; Bilodeau, R. C.; Brodie, C. A.; Haugen, H. K. Systematic study of the stable states of C-, Si-, Ge-, and Sn- via infrared laser spectroscopy. *Phys. Rev. A* **1998**, *58*, 2844–2856.

18 Filler, M. A.; Van Deventer, J. A.; Keung, A. J.; Bent, S. F. Carboxylic acid chemistry at the Ge(100)-2×1 interface: Bidentate bridging structure formation on a semiconductor surface. *J. Am. Chem. Soc.* **2006**, *128*, 770–779.

19 Keung, A. J.; Filler, M. A.; Porter, D. W.; Bent, S. F. Tertiary amide chemistry at the Ge(100)-2×1 surface. *Surf. Sci.* **2005**, *599*, 41–54.

20 Miotto, R.; Ferraz, A. C.; Srivastava, G. P. First-principles study of the adsorption of PH_3 on Ge(001) and Si(001) surfaces. *Braz. J. Phys.* **2002**, *32*, 392–395.

21 Tsai, H.-W.; Lin, D.-S. Comparison of thermal reactions of phosphine on Ge(100) and Si(100) by high-resolution core-level photoemission. *Surf. Sci.* **2001**, *482*, 654–658.

22 Except where otherwise noted, calculations were performed using the Gaussian 03 software package at the B3LYP level of theory. The Si and Ge surfaces were represented by $Si_{15}H_{16}$ and $Ge_{15}H_{16}$ clusters, respectively, containing two adjacent dimers in the same row. Dimer and adsorbate atoms were modeled using the 6-311++G(d,p) basis set; subsurface Ge atoms were modeled using the LANL2DZ pseudopotential; terminal H atoms were modeled using the 6-31G(d) basis set.

23 Ehrley, W.; Butz, R.; Mantl, S. External infrared reflection absorption-spectroscopy of methanol on an epitaxially grown Si(100)-2×1 surface. *Surf. Sci.* **1991**, *248*, 193–200.

24 Lai, Y. H.; Yeh, C. T.; Yeh, C. C.; Hung, W. H. Thermal reactions of methanethiol and ethanethiol on Si(100). *J. Phys. Chem. B* **2003**, *107*, 9351–9356.

25 Bond energy calculations were performed at the B3LYP level of theory using the Gaussian 03 suite of programs. X–H, X–Ge, and X–Si bond energies (X = C, N, P, As, O, S, or Se) were calculated for X–H dissociation of R_nXH (where R is adsorbate-specific and *n* satisfies valence) on the Si and Ge surfaces, which were modeled using $Si(SiH_3)_3$ and $Ge(GeH_3)_3$ clusters, respectively. The bond energy calculations followed the method described in ref 5. All atoms were modeled using the 6-311++G(d,p) basis set.

26 Prayongpan, P.; Michael Greenlief, C. Density functional study of ethylamine and allylamine on Si(100)-2×1 and Ge(100)-2×1 surfaces. *Surf. Sci.* **2009**, *603*, 1055–1069.

27 Pauling, L. Nature of the chemical bond. IV. Energy of single bonds and relative electron negativity of atoms. *J. Am. Chem. Soc.* **1932**, *54*, 3570–3582.

28 Filler, M. A.; Musgrave, C. B.; Bent, S. F. Carbon–oxygen coupling in the reaction of formaldehyde on Ge(100)-2×1. *J. Phys. Chem. C* **2007**, *111*, 1739–1746.

29 Kim, A.; Filler, M. A.; Kim, S.; Bent, S. F. Ethylenediamine on Ge(100)-2×1: The role of interdimer interactions. *J. Phys. Chem. B* **2005**, *109*, 19817–19822.

30 Filler, M. A.; Keung, A. J.; Porter, D. W.; Bent, S. F. Formation of surface-bound acyl groups by reaction of acyl halides on Ge(100)-2×1. *J. Phys. Chem. B* **2006**, *110*, 4115–4124.

31 Filler, M. A.; Mui, C.; Musgrave, C. B.; Bent, S. F. Competition and selectivity in the reaction of nitriles on Ge(100)-2×1. *J. Am. Chem. Soc.* **2003**, *125*, 4928–4936.

32 Keung, A. J.; Filler, M. A.; Bent, S. F. Thermal control of amide product distributions at the Ge(100)-2×1 surface. *J. Phys. Chem. C* **2007**, *111*, 411–419.